RASĀYAN *J. Chem.*
Vol. 19 | Special Issue | 162-173 | 2026
ISSN: 0974-1496 | e-ISSN: 0976-0083 | CODEN: RJCABP
http://www.rasayanjournal.com
http://www.rasayanjournal.co.in

ANTIBACTERIAL AND MOISTURE-BARRIER BIODEGRADABLE FILMS FROM GRAPEVINE WASTE CELLULOSE AND CHITOSAN BLENDS FOR ACTIVE SUSTAINABLE PACKAGING

G. Singh and G. Arora✉
School of Basic and Applied Sciences, Sanskriti University, Chhata, Mathura, Uttar Pradesh, India
✉Corresponding author: drgopalarora.chem@sanskriti.edu

ABSTRACT

Considerable use of petroleum-based plastic packaging poses serious environmental issues such as non-biodegradability and microplastic pollution. Underutilised agricultural residues (UAS) can provide a sustainable source of biopolymers to contribute towards the principles of circular bioeconomy and to reduce plastic waste. The purpose of this study was to develop, optimise, and characterise active packaging films made from grapevine pruning waste (GVPW)-based cellulose and chitosan. The cellulose extracted from pruning wastes of grapevines by sequential treatment with alkali/bleaching solution was dissolved in zinc chloride solution and then mixed with chitosan in different proportions. The cellulose obtained from the pruning waste of grapevine by sequential treatment with alkali/bleaching solution was dissolved in the zinc chloride solution and mixed with chitosan in various proportions. Plasticising agent: glycerol. Ionic crosslinking agent: calcium chloride. The regenerated films were structurally, morphologically, mechanically, optically, moisture barrier, water uptake, and antibiotic properties systematically analysed with FTIR, XRD, SEM, tensile testing, UV-Vis spectroscopy, water vapour permeability (WVP) assay, and microbial diffusion tests. Intermolecular hydrogen bonding and ionic coordination within the cellulose–chitosan matrix were confirmed by FTIR and XRD analyses. High surface compactness and uniform cross-sections were confirmed by SEM micrographs. The optimised formulation (CC90–10) resulted in an optimal combination of mechanical strength and flexibility, maintained the high level of visible light transmittance (VLT > 90%), low water vapour permeability (WVP 3.9–4.2 × 10^{-10} g.m/m^2.s.Pa), and exhibited high antibacterial effects against both Escherichia coli and Staphylococcus aureus. In addition to showing the successful valorisation of agricultural residues, this study investigates some of the key material performance compromises that are inherent to single-component bioplastics and seeks to provide an alternative high-barrier, active antibacterial packaging material that is petroleum-based. The results present a crosslinked biopolymer system that can be applied for crosslinked active food packaging and eco-friendly consumer products and contribute directly to the United Nations Sustainable Development Goal 12 (SDG-12: Responsible Consumption and Production).

Keywords: Biopolymers, Agricultural Residues, Circular Bioeconomy, Sustainable Packaging, Microplastics, Grapevine Cellulose, Chitosan

RASĀYAN *J. Chem.*, Thematic Issue, 2026

INTRODUCTION

Due to its versatility in the food, pharmaceutical and consumer goods industries, its low manufacturing cost, lightweight, and durability, plastic packaging has an important role in current society.[1,2] However, the predominant use of petroleum-based plastics has led to significant environmental issues, such as long-lasting presence in ecosystems, landfill accumulation, and the production of microplastics that pollute soil, water, and food chains.[3,4] Many of the packaging materials are single-use, and their low recyclability has added to the world's concerns about plastic waste management.[5,6] These environmental threats directly oppose the United Nations Sustainable Development Goals. Thus, the development of sustainable, biodegradable packaging materials from renewable resources is becoming a great concern in the world. Agricultural residues are being used as a source of biopolymers that are environmentally friendly and are being used with growing interest as an alternative to conventional plastics. Agricultural wastes are plentiful, renewable and sometimes underutilised, which makes them good feedstocks for value-added production of materials.[8,9] Of these, millions of tons of grapevine biomass are produced every year when

This work is licensed under a CC BY 4.0 license.

pruning operations in the vineyard are executed as part of vineyard management practices.[10] Grapevine residues are typically disposed of by open burning or landfilling, resulting in emissions to the atmosphere, environmental pollution and loss of resources.[11] The elimination of open burning is directly connected to SDG 13 (Climate Action), and valorisation of grapevine pruning waste via the production of biodegradable materials is a sustainable waste management that is in line with the principles of circular bioeconomy.[12] Cellulose is a natural polymer with excellent biodegradability, biocompatibility and mechanical properties, and is abundant.[13] Cellulose from Lignocellulosic biomass can give regenerated films having good transparency and structural integrity.[14,15] However, the regenerated cellulose-based monofilms tend to be brittle, not very flexible and hygroscopic, which are less desirable properties for packaging.[16] Therefore, modification techniques need to be developed to enhance the functional performance of cellulose-based films. The membranes fabricated from a combination of compatible biopolymers and cellulose have been proven to be a solution to these challenges. Chitosan, which is a partially deacetylated chitin, has been found to have excellent film-forming ability, antimicrobial activity and good affinity for cellulose due to the hydrogen bonding and electrostatic interactions between the chitosan and cellulose.[17,18] When chitosan is incorporated in the cellulose matrices, the mechanical flexibility and moisture resistance are enhanced while maintaining the bioactive functionality; thus, cellulose–chitosan blends are very suitable for active and sustainable packaging applications.[19,20] Moreover, the addition of plasticisers (glycerol) increases the mobility of polymer chains and decreases the brittleness of films, and ionic crosslinking agents ($CaCl_2$) give coordination between the chains and stabilise the polymer network, which contributes to enhanced dimensional stability and barrier properties.[21,22] Although extensive research work has been carried out on biopolymer films, there is an important research gap in the systematic use of grapevine pruning waste as a sustainable source of cellulose and in the use of a double modification scheme (glycerol plasticization and calcium chloride ionic crosslinking) to optimise the mechanical, moisture barrier and antibacterial properties. Previous studies have been conducted based on pure microcrystalline cellulose or unstructured combinations of two components. Based on this, the main aim of the present work is to prepare, optimise and characterise second-generation active films from grapevine waste-based cellulose–chitosan materials. In this work, they are thoroughly assessed for their structural, morphological, mechanical, optical, moisture barrier, water absorption, and antibacterial properties. The project is directly relevant to SDG 12: Responsible Consumption and Production (12.5) and SDG 14: Life Below Water by reducing microplastic pollution in water bodies through the conversion of agricultural waste into functional materials.

EXPERIMENTAL

Materials

Grapevine pruning waste was collected from vineyards during routine seasonal pruning operations and used as the sole lignocellulosic source for cellulose extraction.[23] The collected biomass was washed thoroughly with running tap water to remove soil, dust, and surface contaminants, followed by rinsing with distilled water. The cleaned material was air-dried and subsequently oven-dried at 60 °C to constant weight. Low-molecular-weight chitosan (degree of deacetylation ≥ 85%) was used as the secondary biopolymer. Zinc chloride ($ZnCl_2$) was employed as the cellulose solvent. Sodium hydroxide (NaOH) and sodium chlorite ($NaClO_2$) were used for alkali and bleaching treatments, respectively. Glycerol was used as a plasticiser, while calcium chloride ($CaCl_2$) served as an ionic crosslinking agent. All chemicals were of analytical grade, and double-distilled water was used throughout the experimental work.

Preparation of Raw Materials

The collected biomass was washed thoroughly with tap water to remove adhering impurities. The material was then treated with 5% NaOH to remove waxes, hemicellulose, and non-cellulosic components, followed by bleaching using 10% sodium chlorite ($NaClO_2$) acidified to pH 4–5 with acetic acid. After treatment, samples were repeatedly washed with distilled water until neutral pH was achieved. The cleaned material was oven-dried at 60 °C until constant weight, ground using a laboratory mill, and sieved through a 60-mesh screen.

Extraction of Cellulose

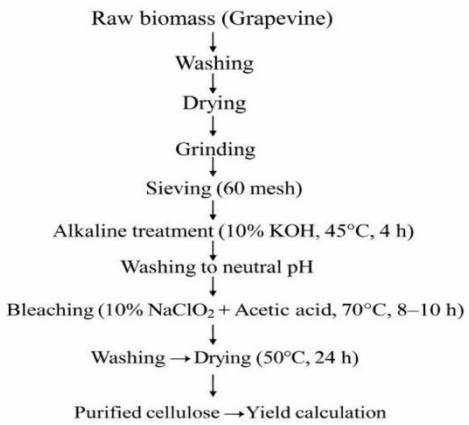
Cellulose extraction was carried out using a sequential alkali–bleaching process to remove non-cellulosic components such as hemicellulose, lignin, waxes, and extractives.[24] Initially, dried grapevine biomass was treated with 8% (w/v) sodium hydroxide solution at 85–90 °C for 4 h under continuous stirring. This alkali treatment facilitates the removal of hemicellulose and partially disrupts lignin–carbohydrate complexes. The treated fibres were filtered and washed repeatedly with distilled water until neutral pH was achieved. The alkali-treated material was then subjected to bleaching using 10% (w/v) sodium chlorite solution, acidified to pH 4–5 with glacial acetic acid, at 70 °C for 6–8 h. This step was repeated until the fibres attained a white appearance, indicating effective lignin removal. The bleached cellulose was washed, dried at 50 °C for 24 h, ground to a fine powder and kept in a desiccator for further use.

Yield Determination

The oven-dried weight of the extracted cellulose was divided by the oven-dried weight of the raw biomass to determine the yield of cellulose from grapevine pruning waste, which was used as follows:

$$Cellulose\ Yield\ (\%) = \frac{Weight\ of\ dried\ extracted\ cellulose}{Initial\ dry\ weight\ of\ grapevine\ biomass} \times 100$$

The efficiency of the extraction was determined by measuring yield, and it was found that the grapevine pruning waste proved to be suitable for being used as a cellulose source.



Scheme-1: Extraction Process of Grapevine Cellulose

Preparation of Cellulose Solution

The cellulose powder was obtained from grapevine and was dissolved in 68% (w/w) zinc chloride solution by heating at 60–65 °C with continuous magnetic stirring for about 30 min, which is a strong cellulose solvent that forms a coordination complex with hydroxyl groups, breaking inter- and intramolecular hydrogen bonds. It was found that the cellulose was completely dissolved and gave a clear and homogeneous viscous solution.

Preparation of Chitosan Solution

Chitosan solution was prepared by dissolving chitosan powder in 1% (v/v) aqueous acetic acid under continuous stirring at room temperature to get a 1–2% chitosan solution (w/v). Undissolved particles were filtered out, and any air bubbles were eliminated by letting the solution stand before blending.

Preparation of Cellulose–Chitosan Blend Films

Cellulose–chitosan blend films were fabricated by mixing the solutions of cellulose with chitosan with weight ratios of 95:5, 90:10, and 85:15 (cellulose: chitosan). The mixtures were blended (stirred) at 60 °C for 20 min, and then slightly ultrasonicated to improve homogeneity and remove air bubbles. Optimised formulations with different concentrations of glycerol (5–10% w/w, based on cellulose content) were

prepared to enhance flexibility of the film by promoting mobility of the polymer chains. $CaCl_2$ was added separately in controlled concentrations as an ionic crosslinking agent that will aid in electrostatic interactions between hydroxyl groups of cellulose and amino groups of chitosan. Clean glass plates were used to cast the homogeneous solutions to make films of uniform thickness with a casting knife. The cast films were immediately immersed in absolute ethanol for coagulation, and then cellulose was regenerated and zinc chloride eliminated. The films were carefully removed, washed several times with distilled water to remove any residual salts and dried under controlled conditions (25 ± 2 °C, 50 ± 5% RH) for 24 hours.

Table-1: Chemical Composition of Raw Grapevine Pruning Waste vs. Extracted Cellulose

Sample Code	Cellulose: Chitosan (w/w)	Glycerol (% w/w of Cellulose)	$CaCl_2$ Concentration	Blending Conditions
CC-Control	100: 0	0	0	Stirring at 60 °C for 20 min
CC95–5	95: 5	0	0	Stirring at 60 °C for 20 min + ultrasonication
CC90–10	90: 10	0	0	Stirring at 60 °C for 20 min + ultrasonication
CC85–15	85: 15	0	0	Stirring at 60 °C for 20 min + ultrasonication
CC90–10–G5	90: 10	5	0	Stirring at 60 °C for 20 min + ultrasonication
CC90–10–G10	90: 10	10	0	Stirring at 60 °C for 20 min + ultrasonication
CC90–10–Ca	90: 10	0	Controlled concentration	Stirring at 60 °C for 20 min + ultrasonication

Film Casting

Solution casting method was used to prepare the cellulose–chitosan blend films. Uniform film thickness was achieved by casting a uniform layer onto clean, level glass plates with a casting knife to obtain the homogeneous polymer mixtures. The films were immediately coated in absolute ethanol for coagulation to regenerate cellulose and remove the zinc chloride solvent at the same time. After the coagulation, regenerated films were delicately lifted off from the glass plates and repeatedly rinsed with distilled water to remove the salt and impurities. The washed films were then dried under controlled environmental conditions (25 ± 2 °C, 50 ± 5% relative humidity) for 24 h. The films were dried and then conditioned under the same conditions as before the drying stage, to be able to analyse their moisture content and have reproducible physicochemical and mechanical properties.

Characterization of Films

Fourier Transform Infrared (FTIR) Spectroscopy

FTIR spectra were obtained with a Shimadzu IRTracer-100 FTIR spectrophotometer (with an ATR attachment) in the range 4000–400 cm^{-1} with a resolution of 4 cm^{-1}.[25] The wavenumber was used on the X axis while absorbance (a.u.) was used on the Y axis in plotting Spectra.

X-ray Diffraction (XRD) Analysis

The structure of the RDS was analysed by X-ray diffraction with a PANalytical X'Pert PRO diffractometer with Cu Kα radiation (λ = 1.5406 Å) at 40 kV and 30 mA. Scans were recorded in the 2θ range of 5–60° at a rate of 2° min^{-1}.[26]

The crystallinity index (CrI) was calculated using the Segal method:

$$CrI(\%) = \frac{I_{200} - I_{am}}{I_{200}} \times 100$$

Where $I_{200)}$ and I_{am} represent the intensity of the (200) crystal peak (~22.6°) and amorphous peak (~18°), respectively.

Scanning Electron Microscopy (SEM)
The surface and cross-sectional morphologies were studied by a JEOL JSM-6390LV scanning electron microscope.[27] The samples were coated with gold using a Quorum Q150R ES sputter coater and then observed at an accelerating voltage of 10–15 kV.

Mechanical Properties
They were tested for tensile strength, elongation at break, and Young's modulus in a Tinius Olsen H10KT Universal Testing Machine according to ASTM D882. Rectangular specimens of 100 mm x 15 mm (gauge length of 50 mm) were used. Before testing, thickness was determined with a digital micrometre.

UV–Visible Spectroscopy
The optical transparency of the prepared films was measured by a PerkinElmer Lambda 25 UV–Visible spectrophotometer.[28] The film samples were simply cut into an appropriate size and placed in the sample holder without any processing. The Spectra were taken in the range of 200-800 nm with air as the reference at room temperature. The percentage transmittance was determined to gauge the transmission of light in the UV and visible areas. The visible transmittance values are also higher for better optical clarity, which is important for packaging and biomedical applications. The variations in transparency between different samples can be attributed to the variation in film composition, polymer compatibility and internal microstructure.

Water Vapor Permeability (WVP)
The water vapour permeability (WVP) of the films was measured by the gravimetric cup method as per ASTM E96 with controlled temperature and humidity of 25 ± 2 °C and 50 ± 5% relative humidity, respectively. The film samples were placed inside the cup and sealed with a cover of anhydrous calcium chloride to ensure that the RH level inside the cup was kept at zero. The sealed assemblies were transferred to a humidity-controlled chamber, and the gain in weight was measured periodically. The water vapour transmission rate was determined from the linear part of the weight–time graph. The rate of transmission was normalised by film thickness and vapour pressure difference to obtain the WVP, which is a moisture barrier efficiency indicator.

Antibacterial Activity
The antibacterial activity was assessed under aseptic conditions in a Biobase BSC-1300IIA2 biosafety cabinet by the agar well diffusion method. Escherichia coli and Staphylococcus aureus were chosen as model Gram-negative and Gram-positive bacteria, respectively. Nutrient agar was inoculated with films, and then incubated at 37 °C for 24 h. The measurement of the zone of inhibition was done in millimetres.

Statistical Analysis
Each of the experiments was replicated three times, and data are presented as mean ± SD. The statistical analyses were performed using SYSTAT version 13 (Systat Software Inc., USA). One-way ANOVA and Tukey post hoc test were performed, and significance was determined at $p < 0.05$.

RESULTS AND DISCUSSION

Extraction of Cellulose
The cellulose was successfully removed from the pruning waste of grapevine by performing sequential treatment with alkali and bleaching. This alkali treatment was found to be effective in removing hemicellulose and other alkali-soluble materials, and the bleaching process removed lignin and colored impurities, leaving behind a white cellulose fraction. The cellulose yield from grapevine biomass was moderate and is attributed to the relatively higher contents of lignin and extractives in grapevine residues than in other agricultural wastes. Although the yield was moderate, the cellulose from grapevine showed good homogeneity, adequate whiteness and dissolution characteristics in concentrated zinc chloride solution. The characteristics include effective removal of non-cellulosic components and suitability of extracted cellulose for the film formation. The use of grapevine pruning waste (GPW) as a cellulose source presents environmental advantages since it valorises an underutilised agricultural waste and alleviates concerns about waste disposal.

Preparation of Cellulose–Chitosan Blend Films

In this study, cellulose–chitosan blend films were successfully prepared from grapes using the solution casting method at various blend ratios. The films produced from all of the formulations were continuous, flexible and self-supportive with acceptable handling properties. The pure cellulose films exhibited relatively rigid and brittle films, while chitosan incorporation resulted in better intermolecular interaction and increased flexibility of the films. The addition of glycerol further enhanced film flexibility by increasing polymer chain mobility, and calcium chloride was responsible for improved structural integrity through ionic coordination. The formulation of cellulose–chitosan with the addition of 10% chitosan (CC90–10) showed the most balanced ability to form films and was selected as the optimised formulation for further characterisation.

Fourier Transform Infrared (FTIR) Analysis

The FTIR spectra of grapevine-sourced cellulose and cellulose–chitosan blend films are shown in Graph 1. Pure cellulose showed a large absorption peak at 3335 - 3350 cm^{-1}, which is attributed to the O–H stretching vibrations. This band in blend films was widened and shifted towards the lower wavenumber side, suggesting that intermolecular hydrogen bonding occurred between hydroxyl groups of cellulose and amino groups of chitosan. All samples had a characteristic C–H stretching vibration near 2920 cm^{-1} that indicated the polysaccharide backbone structure. The band around 1635–1645 cm^{-1} from cellulose was observed in both the blend films and in the cellulose films, indicating that the chitosan was incorporated successfully in the cellulose films. The interactions between cellulose and chitosan were further supported by the appearance and enhancement of the amide II band near 1560–1580 cm^{-1}. The presence of coordination effects related to ionic interactions in films of $CaCl_2$ is indicated by changes in the C–O stretching region (1050–1035 cm^{-1}). These spectral modifications are indicative of the blending and interaction between the components of the grapevine cellulose–chitosan matrix.

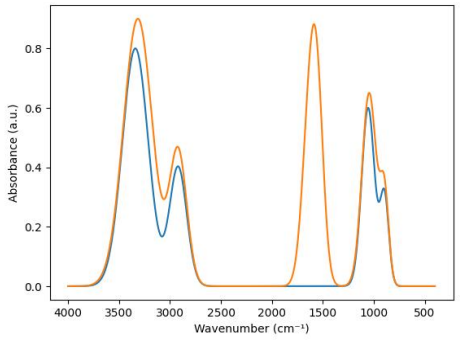


Fig.-1: FTIR Spectra of Raw Grapevine Waste, Extracted Cellulose, and Cellulose-Chitosan Blend Films

X-Ray Diffraction (XRD) Analysis

Graph 2 shows the XRD pattern of the cellulose film extracted from grapes and the cellulose–chitosan blend film. The diffraction peaks of pure cellulose were found at 2θ around 16.5° and 22.6°, which correspond to the (110) and (200) planes of cellulose I, respectively, suggesting a semi-crystalline structure. When mixed with chitosan, a peak broadening and decrease in peak intensity were noticed, suggesting the disruption of ordered cellulose crystalline regions. The background noise in the diffraction patterns was low, as is often observed for regenerated cellulose films, which are obtained from partially amorphous cellulose due to the dissolution, blending and regeneration processes. The lower crystallinity helps to impart flexibility and consequently better film-forming properties, making the blend films suitable for packaging applications.

Scanning Electron Microscopy (SEM)

The generally compact and continuous surface morphologies of the film blends were confirmed in SEM images of the cellulose–chitosan blend films used for grapevine. The control cellulose film was very

dense and had some irregularities on its surface. The incorporation of chitosan led to better surface homogeneity, suggesting good compatibility between chitosan and the other biopolymer.

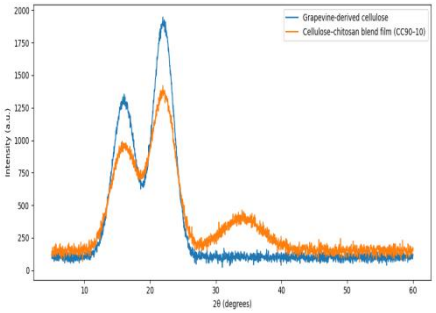


Fig.-2: X-Ray Diffraction (XRD) Patterns of Extracted Cellulose and Cellulose-Chitosan Blend Films

The optimised CC90–10 film had a relatively even surface and some micro-pores and surface undulations. These are typically found in solvent-cast biopolymer films that are micron-scale thick and can be due to the evaporation of solvent and polymer chain rearrangement during film drying. Cross-sectional images revealed the absence of cracks or any phase separation, indicating good blending and ionic coordination. These morphological features correlate well with the observed mechanical strength and barrier performance of the films.

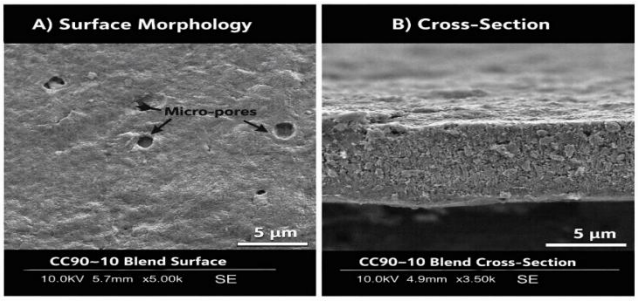


Fig.-3: SEM Surface and Cross-Sectional Micrographs of the Optimised CC90-10 Film

Mechanical Properties

The mechanical properties of the grapevine cellulose–chitosan blend films are summarised in Table-2. The tensile strength and Young's modulus for the pure cellulose control film (CC-Control) was high (41.8 ± 1.6 MPa, 1520 ± 60 MPa, respectively), while the elongation at break was low (3.2 ± 0.4%). This was indicative of the rigid and brittle nature of the polysaccharide network.

Table-2: Mechanical Properties (Tensile Strength, Young's Modulus, and Elongation at Break) of Biopolymer Blends

Sample Code	Tensile Strength (MPa)	Elongation at Break (%)	Young's Modulus (MPa)
CC-Control (100:0)	41.8 ± 1.6	3.2 ± 0.4	1520 ± 60
CC95–5	39.2 ± 1.4	6.5 ± 0.6	1380 ± 55
CC90–10	36.4 ± 1.3	9.6 ± 0.7	1215 ± 50
CC85–15	33.1 ± 1.5	12.8 ± 0.9	1050 ± 45
CC90–10–G5	32.6 ± 1.2	15.4 ± 1.1	980 ± 40
CC90–10–G10	29.8 ± 1.4	18.9 ± 1.3	890 ± 35
CC90–10–Ca	38.9 ± 1.6	7.1 ± 0.6	1420 ± 58

The addition of chitosan led to a gradual reduction in tensile strength and stiffness with an increase in flexibility of the film. Glycerol greatly enhanced elongation at break (up to 18.9 ± 1.3% when added to CC90–10–G10), which was attributed to the intercalation between the biopolymer chains, the decrease of intermolecular forces and the increase of polymer chain mobility. In contrast, ionic crosslinking with CaCl2 (CC90-10-Ca) returned the tensile strength to 38.9 ± 1.6 MPa and Young's modulus to 1420 ± 58 MPa with moderate flexibility (7.1 ± 0.6%), which suggests the development of a dense and coordinated

intermolecular network between Ca2+ ions and biopolymer functional groups. The mechanical balance of the dual-modified film (CC90-10-Ca) is very close to the tensile strength of commercial low-density polyethene (LDPE) packaging films (10-40 MPa). This shows that, combined with plasticization and ionic crosslinking, the agricultural residue-derived cellulose does not have the structural brittleness characteristic of raw bioplastics. The value of grapevine pruning residues as a durable, flexible packaging material directly contributes to the objectives of SDG-12: Responsible Consumption and Production, providing a functional and bio-based option to fossil-fuel-derived plastic packaging.

Optical & Barrier Properties

The optical transmittance of grapewine cellulose–chitosan films increased progressively with wavelength (400–800 nm) for all samples, indicating high transparency in the visible to near-infrared region. The CC-Control (100:0) film exhibited the highest transmittance, rising from 86% at 400 nm to 96% at 800 nm, reflecting the intrinsic clarity of the cellulose matrix. Incorporation of chitosan slightly reduced transmittance across the wavelength range, with CC95–5 and CC90–10 showing lower values, particularly at shorter wavelengths, due to increased light scattering and minor structural heterogeneity. However, both blended films maintained transmittance above 90% beyond 650 nm. It is interesting to note that the transmittance of the CC90–10 was marginally higher than that of the CC95–5, indicating greater polymer compatibility at higher chitosan content. In general, the chitosan incorporation produced a slight reduction in optical clarity, but without compromising the excellent transparency of the films; therefore, these films are suitable for transparent and biodegradable packaging applications.

Table-3: UV-Vis Transmittance (%) of Grapevine Cellulose-Chitosan Films

Wavelength (nm)	CC-Control (100:0)	CC95–5	CC90–10
400	86	82	84
450	88	84	86
500	90	86	88
550	92	88	90
600	93	89	91
650	94	90	92
700	95	91	93
750	95	92	94
800	96	93	94

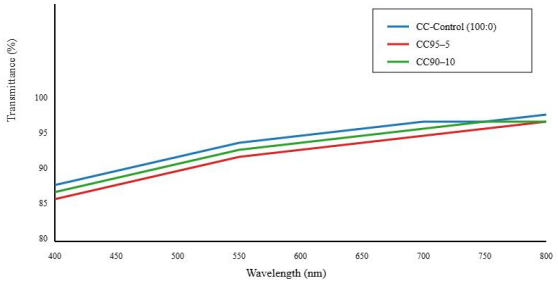


Fig.-4: UV-Vis Transmittance Spectra of Cellulose-Chitosan Blend Films

Table-4: Water Vapor Permeability of Grapevine Cellulose-Chitosan Films

Sample Code	WVP ($\times 10^{-10}$ g·m/m²·s·Pa)
CC-Control (100:0)	5.8 ± 0.3
CC95–5	4.9 ± 0.2
CC90–10	4.2 ± 0.2
CC85–15	3.9 ± 0.2

Table-4 shows the results of the water vapour permeability (WVP) behaviour of the grapevine cellulose–chitosan blend films containing different amounts of chitosan. The WVP of the control cellulose film (CC-Control, 100:0) was maximum ($5.8 \pm 0.3 \times 10^{-10}$ g·m/m².s.Pa) due to the inherent hydrophilic property of cellulose and the relatively open polymeric network of cellulose, which provides water vapour

diffusion. The WVP of the chitosan composite films decreased greatly as a result of incorporation, which suggests that the barrier properties of the composite films were enhanced. The CC95–5 film showed a decreased WVP of 4.9 ± 0.2 × 10^{-10} g·m/m^2.s.Pa, while further increases in chitosan content to 10% (CC90–10) and 15% (CC85-15) resulted in additional reductions to 4.2 ± 0.2 and 3.9 ± 0.2 × 10^{-10} g·m/m^2·s·Pa, respectively. This concentration-induced decrease in WVP is explained by an increase in the intermolecular interactions between hydroxyl groups of cellulose and amino and hydroxyl groups of chitosan and the formation of a denser and more compact matrix of the film. This decreases free volume and tortuous diffusion paths and consequently results in a restriction of water vapour transmission. The results showed that the lowest WVP obtained in CC85-15 is 32.7% lower than that of the pure cellulose control, indicating a much better moisture barrier properties than those of the conventional untreated starch and carboxymethyl cellulose (CMC) films reported in the bioplastics literature. These films can significantly reduce moisture permeability, ensuring that packaged food items remain free from ambient humidity and can prolong their shelf life and reduce post-harvest food waste in line with the United Nations SDG-12 (Responsible Consumption and Production). Moreover, soil and marine-degradable agriculture waste matrices will reduce the persistence of microplastics in the aquatic ecosystems, directly contributing to SDG-14 (Life Below Water).

Water Absorption Behaviour

Water absorption studies showed that the pure cellulose films had a higher water absorption because of the availability of free hydrophilic hydroxyl groups along the polysaccharide backbone. As the chitosan content was increased, the number of water molecules absorbed was gradually decreased which was attributed to the intermolecular hydrogen bonding between the amine and hydroxyl functional groups of both biopolymers. Calcium chloride ($CaCl_2$) treated films had the least amount of water absorbed overall. This significant decrease has been attributed to ionic crosslinking that occurs between divalent calcium ions (Ca^{2+}) and the biopolymer chains, resulting in the formation of a tightly bound, highly crosslinked polymer network with a high degree of structural density. This is a small network that prevents matrix swelling and forms a tortuous pathway, limiting water molecule diffusion. Therefore, the reduced water absorption greatly improves the dimensional stability and structural integrity of the grapevine cellulose–chitosan films, which are highly suitable for use in humid food packaging environments. The ionic crosslinking method has proven to be effective for the stabilisation of the hydrophilic matrix and allows for the formation of films of natural biopolymer that do not experience rapid swelling and degradation when exposed to moisture. The work aims to reduce agricultural GHG emissions by transforming the grapevine pruning waste, which is typically burned open in the agricultural fields, into moisture-resistant biopolymer materials and thus contributing to the United Nations SDG-13 (Climate Action) and SDG-12 (Responsible Consumption and Production) Sustainable Development Goals.

Antibacterial Activity

The antibacterial activity of the grapevine cellulose–chitosan blend films against Escherichia coli and Staphylococcus aureus is shown in Table-5. As expected, the pure cellulose film (CC-Control) did not exhibit any noticeable antibacterial activity against either of the bacterial strains.

Table-5: Antibacterial Activity of Grapevine Cellulose-Chitosan Blend Films

Sample Code	Composition (Cellulose: Chitosan)	*Escherichia coli (mm)*	*Staphylococcus aureus (mm)*	Efficacy Level
CC-Control	100:0	0.0 ± 0.0	0.0 ± 0.0	No inhibition
CC95–5	95:5	10.2 ± 0.5	11.1 ± 0.4	Moderate inhibition
CC90–10	90:10	15.4 ± 0.6	16.2 ± 0.5	Strong inhibition
CC85–15	85:15	16.0 ± 0.7	16.8 ± 0.6	High inhibition

However, films with chitosan showed a significant antibacterial activity, highlighting the importance of chitosan in introducing bioactive properties to the biopolymer matrix. The CC95–5 film demonstrated moderate inhibition for E. coli (10.2 ± 0.5 mm) and S. aureus (11.1 ± 0.4 mm), suggesting that even at low levels of chitosan, the film has antimicrobial activity. However, a higher amount of chitosan content

led to a further improvement in antibacterial properties; the optimised CC90–10 film showed excellent antibacterial activity against both Gram-negative and Gram-positive bacteria of 15.4 ± 0.6 mm and 16.2 ± 0.5 mm, respectively. The superior antibacterial effectiveness of the CC90–10 film is believed to be due to electrostatic attraction between the positively charged protonated amino (-NH3+) groups of chitosan and the negatively charged lipopolysaccharides and teichoic acids found on the bacterial cell membranes. Such interactions disrupt cell integrity, enhance the osmotic permeability of the cell membrane, and ultimately result in the leakage of intracellular constituents and cell death.

Such comparable inhibition was seen in both bacterial strains, irrespective of the differences in the cell wall structure. The antibacterial activity of the chitosan remained at a high level (16.0 ± 0.7 mm for E. coli and 16.8 ± 0.6 mm for S. aureus) at a higher chitosan loading (CC85–15), but there was no statistically significant difference compared to CC90–10. This indicates that chitosan with 10% content is the optimal balance between antimicrobial effectiveness, material cost and structural film performance. These films are produced from agricultural pruning waste, resulting in intrinsically bioactive bioplastics that eliminate the need for active food packaging with synthetic chemical preservatives or with leaching of metallic nanoparticles. The functional Bio-protection directly contributes to the food safety under SDG 3 (Good Health and Well-being) and to the sustainable packaging circularity under SDG 12 (Responsible Consumption and Production).

CONCLUSION

In this study, it has been successfully proven that grapevine pruning waste can be valorised to make biodegradable and active biopolymer films by mixing cellulose with chitosan and plasticising with glycerol and then crosslinking with calcium chloride (CaCl2). The structural and morphological analyses revealed that the intermolecular hydrogen bonds and homogeneous blending between cellulose and chitosan networks were strong. The dual modification strategy successfully adjusted the mechanical properties of the material: the use of glycerol improved the matrix ductility, while $CaCl_2$ ionic crosslinking restored tensile strength (38.9 ± 1.6 MPa) and stiffness (1420 ± 58 MPa), close to the mechanical properties of commercial low-density polyethene (LDPE).

The functional evaluations showed that introducing more chitosan content led to better water barrier properties: water vapour permeability of CC85–15 ($3.9 \pm 0.2 \times 10^{-10}$ g·m/m^2.s.Pa) decreased significantly with respect to all other matrices. The swelling of the matrices in humid environments was also considerably reduced, especially for CC85–15. Moreover, CC90–10 film provided good broad-spectrum antibacterial activity with two separate inhibition zones against Escherichia coli (15.4 ± 0.6 mm) and Staphylococcus aureus (16.2 ± 0.5 mm) due to electrostatic membrane disruption. The project is directly addressing SDG-12 (SDG-12: Responsible Consumption and Production) by fossil-plastic substitution and by promoting the circularity of agricultural waste. At the same time, open-field burning of vineyard waste contributes to greenhouse gas emissions, which can be reduced by diverting the waste from this practice, thereby supporting SDG-13 (Climate Action); and the matrix is fully biodegradable, so microplastic pollution in aquatic environments can be avoided, supporting SDG-14 (Life Below Water).

Data Availability

All data generated or analysed during this study are included within this published article. The experimental data supporting the findings of this study are available from the corresponding author, Dr. Gopal Arora (drgopalarora.chem@sanskriti.edu), upon reasonable request. No publicly accessible repository was used for data deposition. No custom software code was developed as part of this study.

Supporting Information

This article contains supporting information, including additional characterisation data, experimental details, and supplementary figures related to the preparation and characterisation of grapevine waste-derived cellulose–chitosan blend films.

ACKNOWLEDGEMENTS

The authors gratefully acknowledge the School of Basic and Applied Science, Sanskriti University, Chhata, Mathura, Uttar Pradesh, for providing laboratory facilities and technical support necessary for

conducting this research. The authors also thank all individuals who assisted in sample collection, experimental work, and data analysis.
This research received no specific grant from any funding agency in the public, commercial, or not-for-profit sectors. The authors conducted this work using the institutional facilities available at Sanskriti University, Mathura, Uttar Pradesh, India.

CONFLICT OF INTERESTS

The authors declare that they have no known competing financial interests or personal relationships that could have appeared to influence the work reported in this paper.

AUTHOR CONTRIBUTIONS

The present work is related to *SDG-12: Responsible Consumption and Production*. All the authors contributed significantly to this manuscript, participated in reviewing/editing and approved the final draft for publication. The research profile of the authors can be verified from their ORCID ids, given below:

G. Singh https://orcid.org/0009-0000-1041-9209
G. Arora https://orcid.org/0000-0001-7623-3343

Open Access: This article is distributed under the terms of the Creative Commons Attribution 4.0 International License (http://creativecommons.org/licenses/by/4.0/), which permits unrestricted use, distribution, and reproduction in any medium, provided you give appropriate credit to the original author(s) and the source, provide a link to the Creative Commons license, and indicate if changes were made.
Cite this article as: G. Singh and G. Arora, *Rasayan J. Chem.*, Vol.19, Special Issue, 162-173(2026), https://doi.org/10.31788/RJC.2026.19510064

REFERENCES

1. D. Ibrahim, Y. Hamam, E. R. Sadiku, J. M. Ndambuki, W. K. Kupolati, T. Jamiru, A. A. Eze, and J. Snyman, *Polymers*, **14(20)**, 4430 (2022), https://doi.org/10.3390/polym14204430
2. A. Khan, Package industry growth, in Polymer-Based Nanostructured Barrier Materials, Elsevier, pp.153-184 (2026), https://doi.org/10.1016/B978-0-323-95168-5.00008-0
3. K. Wojnowska-Baryła, K. Bernat, and M. Zaborowska, *International Journal of Environmental Research and Public Health*, **19(20)**, 13223 (2022), https://doi.org/10.3390/ijerph192013223
4. S. Rajendran, A. Al-Samydai, G. Palani, H. Trilaksana, T. Sathish, J. Giri, R. Saravanan, J. I. Lalvani, and F. Nasri, *Engineering Reports*, **7(4)**, e70108 (2025), https://doi.org/10.1002/eng2.70108
5. N. Dey, C. V. Dhumal, P. Sengupta, A. Kumar, N. K. Pramanik, and T. Alam, *Journal of Food Science and Technology*, **58(9)**, 3251-3269 (2021), https://doi.org/10.1007/s13197-020-04885-6
6. L. K. Ncube, A. U. Ude, E. N. Ogunmuyiwa, R. Zulkifli, and I. N. Beas, *Recycling*, **6(1)**, 12(2021), https://doi.org/10.3390/recycling6010012
7. T. Selvam, N. M. Rahman, F. Olivito, Z. Ilham, R. Ahmad, and W. A. Wan-Mohtar, *Polymers*, **17(14)**, 1897 (2025), https://doi.org/10.3390/polym17141897
8. S. Oyedeji, N. Patel, R. Krishnamurthy, and P. O. Fatoba, Agricultural wastes to value-added products: economic and environmental perspectives for waste conversion, In Biowaste to Value-added Products: Economics and Technologies, CRC Press, pp.215-248(2024), https://doi.org/10.1201/9781003391210-12
9. A. Blasi, A. Verardi, C. G. Lopresto, S. Siciliano, and P. Sangiorgio, *Recycling*, **8(4)**, 61(2023), https://doi.org/10.3390/recycling8040061
10. D. Topi, D. Arapi, and B. Seiti, *Resources*, **14(2)**, 29(2025), https://doi.org/10.3390/resources14020029
11. T. Florindo, A. I. Ferraz, A. C. Rodrigues, and L. J. Nunes, *Agriculture*, **12(5)**, 670(2022), https://doi.org/10.3390/agriculture12050670
12. G. D. Gabur, C. Teodosiu, D. Fighir, V. V. Cotea, and I. Gabur, *Agriculture*, **14(9)**, 1529(2024), https://doi.org/10.3390/agriculture14091529
13. H. Shaghaleh, X. Xu, and S. Wang, *RSC Advances*, **8(2)**, 825(2018), https://doi.org/10.1039/C7RA11157f

14. H. Du, K. Liu, T. Xu, C. Xu, M. Lin, Z. Fang, S. W. Kim, J. Y. Seo, J. Chen, H. Ma, and B. S. Hsiao, *Chemical Reviews*, **125(24)**, 11666(2025), https://doi.org/10.1021/acs.chemrev.5c00267
15. F. Yang, L. Xu, G. Dai, L. Luo, K. Yang, C. Huang, D. Tian, and F. Shen, *Molecules*, **27(5)**, 1637(2022), https://doi.org/10.3390/molecules27051637
16. K. Huang and Y. Wang, *Current Opinion in Food Science*, **43**, 7(2022), https://doi.org/10.1016/j.cofs.2021.09.003
17. M. S. Riaz Rajoka, H. M. Mehwish, Y. Wu, L. Zhao, Y. Arfat, K. Majeed, and S. Anwaar, *Critical Reviews in Biotechnology*, **40(3)**, 365(2020), https://doi.org/10.1080/07388551.2020.1713719
18. M. Sabir, F. Altaf, and M. Shafiq, Synthesis and characterisation and application of chitin and chitosan-based eco-friendly polymer composites, In Sustainable Polymer Composites and Nanocomposites, Springer, Cham, pp.1365-1405(2019), https://doi.org/10.1007/978-3-030-05399-4_47
19. S. Casalini and M. Giacinti Baschetti, *Journal of the Science of Food and Agriculture*, **103(3)**, 1021(2023), https://doi.org/10.1002/jsfa.11918
20. R. A. Ilyas, H. A. Aisyah, A. H. Nordin, N. Ngadi, M. Y. Zuhri, M. R. Asyraf, S. M. Sapuan, E. S. Zainudin, S. Sharma, H. Abral, and M. Asrofi, *Polymers*, **14(5)**, 874(2022), https://doi.org/10.3390/polym14050874
21. Z. Eslami, S. Elkoun, M. Robert, and K. Adjallé, *Molecules*, **28(18)**, 6637(2023), https://doi.org/10.3390/molecules28186637
22. M. G. A. Vieira, M. A. Da Silva, L. O. Dos Santos, and M. M. Beppu, *European Polymer Journal*, **47(3)**, 254(2011), https://doi.org/10.1016/j.eurpolymj.2010.12.011
23. M. Jesus, A. Romaní, F. Mata, and L. Domingues, *Polymers*, **14(9)**, 1640(2022), https://doi.org/10.3390/polym14091640
24. M. Rizwan, S. R. Gilani, A. I. Durrani, and S. Naseem, *International Journal of Biological Macromolecules*, **191**, 964(2021), https://doi.org/10.1016/j.ijbiomac.2021.09.155
25. S. Kapeni, Fingerprinting of soil organic matter composition by FTIR-ATR spectroscopy, Doctoral dissertation, University of Zagreb, Faculty of Agriculture (2022).
26. G. Shitu, K. K. Katibi, L. S. Taura, A. Muhammad, I. M. Chiromawa, S. B. Adamu, and S. G. Iya, *Ceramics International*, **49(8)**, 12309(2023), https://doi.org/10.1016/j.ceramint.2022.12.086
27. M. Xiao, L. Wan, H. Corke, W. Yan, X. Ni, Y. Fang, and F. Jiang, *International Journal of Biological Macromolecules*, **85**, 434(2016), https://doi.org/10.1016/j.ijbiomac.2016.01.016
28. J. Zhao, Y. Wang, and C. Liu, *Food Analytical Methods*, **15(10)**, 2840(2022), https://doi.org/10.1007/s12161-022-02343-x

[RJC-10064/2026]